21st International Conference on Pattern Recognition (ICPR 2012)
November 11-15, 2012. Tsukuba, Japan

MRI Segmentation of Brain Tissue Based on Spatial Prior and Neighboring Pixels Affinities

Zhanpeng Zhang[1,2], Qingsong Zhu[1,*], Yaoqin Xie[1]
[1]*Shenzhen Institutes of Advanced Technology, Chinese Academy of Sciences, Shenzhen, China*
[2]*Sun Yat-Sen University, Guangzhou, China*
E-mails: {zp.zhang, qs.zhu, yq.xie}@siat.ac.cn

Abstract

Segmentation of brain tissue in magnetic resonance imaging (MRI) can identify anatomical areas of interest. It has been widely used in medical imaging applications. In this paper, we propose a new brain MRI segmentation method, which takes advantage of spatial prior and neighboring pixels affinities. In addition, the underlying model can naturally describe the partial volume effects. Firstly, the algorithm labels some pixels based on pixel intensity and spatial prior. The label information is then propagated from the labeled pixels to unlabeled pixels with neighboring pixels affinities. Mathematically, the result is obtained by minimizing a quadratic objective function. In this way, we can extract different types of brain tissue from MR images and obtain the segmentation result. Experiments prove that our method can generate accurate results, which are comparable to that of the state-of-the-art methods.

1. Introduction

MRI segmentation of brain tissue is widely applied to identify anatomical areas of interest for diagnosis, treatment, surgical planning and image registration. Specifically, the brain tissue segmentation usually refers to the problem of classifying each pixel (voxel) into one of the following tissue types: Gray Matter (GM), White Matter (WM) and Cerebro-Spinal Fluid (CSF). It is an important topic and attracts much research.

Considerable progress on this problem has been reported in existing literatures. Many existing algorithms use parametric models to describe the probability distribution of the tissue features. Mixtures of Gaussians are usually applied to model the tissue intensity [1, 2]. The parameters of the model can be estimated with maximum-likelihood or maximum a posteriori technique. However, as the appearance of the brain tissue is usually complex and the image noise is unavoidable, the algorithms usually have to estimate sophisticated models. There are usually many parameters and the results may be sensitive to the initialization of the parameters. To avoid these problems, some algorithms use non-parametric clustering methods to classify the voxels in the feature space. Representative methods include the use of mean-shift [3]. This kind of methods can avoid the model assumptions in the parametric methods. Besides these methods, active contours, level sets and Markov Random Field [4], are also applied in this problem. These methods are usually reduced to minimizing an energy function, which can take account of the tissue homogeneity, shape of the boundary and other prior knowledge. Recently, learning techniques like support vector machine and random decision forests are also employed [5, 6]. Atlases, the segmented images of the subjects, are also incorporated in the many algorithms [7, 8]. The segmentation can be reduced to a registration problem in which the labels in the atlases are transferred to the target image after the mapping between the atlases and the image is determined. The atlases can also be used to form the probability maps of the tissue, providing spatial prior to enable automatic segmentation or improve the robustness of the algorithms.

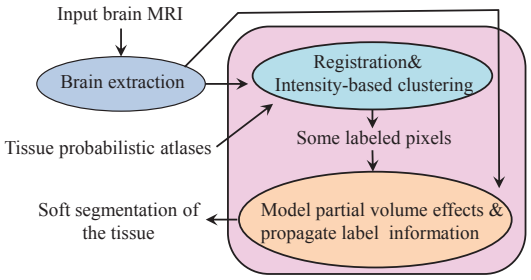

Figure 1. Flow chart of the proposed method.

However, recent algorithms usually aim to capture a global description of the tissue's characteristics, which is difficult as the brain images are complex and the qual-

ity of the local regions in MRI is strongly affected by the imperfection of the imaging devices (e.g., noise, bias). Meanwhile, some algorithms cannot model the partial volume effects naturally, which is common in MRI.

In this paper, we propose a new method for brain tissue segmentation in MRI based on spatial prior and neighboring pixels affinities. Firstly, the algorithm uses spatial prior and intensity-based clustering information to select some pixels and label them as GM, WM, or CSF. After that, we use a linear combination model to describe the pixel intensity to capture the partial volume effects. Under this model, we extract the tissue by propagating the label information to the unlabeled regions with neighboring pixels affinities, which are based on a local smoothness assumption. The extraction results can be obtained by minimizing a quadratic objective function. Due to the modeling of partial volume effects, the extraction results are fractional instead of binary. These soft segmentation results can be treated as the likelihood that a pixel belonging to a certain tissue type and we can obtain the final segmentation result. Fig. 1 shows the flow chart of our proposed method.

2. Methodology

2.1. Labeling pixels based on spatial prior

For the input MRI data, if it contains non-brain structures, we first conduct brain extraction as preprocessing (we use brain extraction tool in FSL [9] in current implementation). After that, we need some initial tissue label information to enable automatic segmentation.

Firstly, we apply a registration step between the MR brain volume and the tissue probabilistic atlases, to get the corresponding prior probability maps. In practice, we carry out this procedure with the SPM8 software package [10]. Then we can obtain the spatial prior knowledge of the tissue from the corresponding prior probability maps (as in Fig. 2). These maps represent the prior probability of a pixel being GM, WM, or CSF (i.e., $P((x, y)|T), T = \{\text{GM, WM, CSF}\}$, where (x, y) is the location of a pixel). Meanwhile, we estimate tissue intensity probability distribution $P(I|T)$ with the prior probability maps. Specifically, we simply use histograms to model the distributions (as shown in Fig. 2) to avoid the limitations of the parametric models. However, distributions of different tissue types inevitably overlap partially. This is because the values in the probability maps change smoothly and are inconsistent with the details of the tissue's shape. To represent the more detailed characteristics, we use intensity-based fuzzy c-means clustering to softly classify the pixels into GM, WM or CSF. So we can obtain the tissue likelihood of

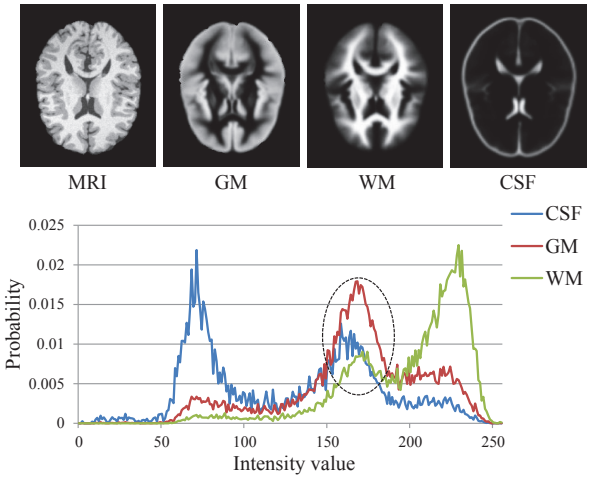

Figure 2. Top: The brain MRI and the corresponding prior probability map of GM, WM and CSF respectively. Bottom: Intensity probability distribution of the above MRI. The ellipse indicates that the distributions overlap.

a pixel i (i.e., $P'(T|i)$). Combining the spatial prior, tissue intensity distribution and the clustering-based tissue likelihood, under the Bayes' rule, we formulate the likelihood of a pixel i being tissue T_m as:

$$\begin{aligned} P(T_m|i) &= P(T_m|I_i, (x_i, y_i)) \\ &= \frac{P(I_i, (x_i, y_i)|T_m)P(T_m)}{\sum_{n=1}^{3} P(I_i, (x_i, y_i)|T_n)P(T_n)} \end{aligned} \quad (1)$$

where $P(I_i, (x_i, y_i)|T_m) = P((x_i, y_i)|T_m)P(I_i|T_m)$. It can be computed by the spatial prior and tissue intensity distribution we estimated before. For $P(T_m)$, we use clustering-based tissue likelihood $P'(T_m|i)$. We compute $P(T_m|i)$ for every pixel i and tissue m. A pixel is then labeled as tissue T_m if $P(T_m|i) > \tau$ (we set $\tau = 0.9$).

2.2. Modeling partial volume effects

Due to the limited resolution of the images, some pixels (especially those near the edges), contain material from multiple tissue types. To achieve high-accuracy result, we model the partial volume effects in our underlying model. By assuming that every pixel i contains at most two different tissue types, we use a linear combination model to describe the mixing effects:

$$I_i = \alpha_i A_i + (1 - \alpha_i) B_i \quad (2)$$

where α_i is the mixing factor. A_i and B_i are the intensities of the underlying tissue types. But there are more than one possible combination of the tissues types. So we extract GM, WM and CSF respectively instead of in a simultaneous mode. For example, when we extract GM, A_i is the intensity of GM and B_i represent that of any other tissue. The solution α_i is then treated as the likelihood of a pixel i being GM.

2.3. Propagating the label information

Equation (2) is under constrained since there are only one known variable (I_i) but three unknown variables (α_i, A_i, B_i). To solve this equation, we can use the labeled pixels as constraints and propagate the label information with pixels affinities. Specifically, we can assume that the intensity values A and B change smoothly respectively and keep constant in a small neighborhood. Under this assumption, Levin *et al.* [11] derive a cost function and show that A and B can be analytically eliminated and obtain a quadratic cost function in α. By applying this method, we can obtain a closed form solution of α with the labeled pixels as constraints. Mathematically, under the local smooth assumption, we can rewrite equation (2) as:

$$\alpha_i \approx aI_i + b, \forall i \in w \tag{3}$$

where $a = \frac{1}{A-B}, b = \frac{-B}{A-B}$ and w is a small window (e.g., 3×3 neighborhood). To obtain a solution obeying the smooth assumption, the cost function is as follows:

$$J(\alpha, a, b) = \sum\nolimits_{j \in P} \left(\sum\nolimits_{i \in w_j} \left(\alpha_i - a_j I_i - b_j \right)^2 + \varepsilon a_j^2 \right) \tag{4}$$

P is the pixel set of the image. w_j is a small window around pixel j. εa_j^2 is a regularization term. a and b can be analytically eliminated from equation (4)[11], yielding a quadratic cost in α:

$$J(\alpha) = \alpha^T L \alpha \tag{5}$$

Here α is treated as a $|P| \times 1$ vector. L is a $|P| \times |P|$ matrix with the (i, j)-th element as:

$$\sum\nolimits_{k|(i,j) \in w_k} \left(\delta_{ij} - \frac{1}{|w_k|} \left(1 + \frac{(I_i - \mu_k)(I_j - \mu_k)}{\frac{\varepsilon}{|w_k|} + \sigma_k^2} \right) \right) \tag{6}$$

where δ_{ij} is the Kronecker delta. $|w_k|$ is the number of pixels in this window. μ_k and σ_k^2 are the mean and variance of the intensities in the window w_k.

Combined with constraints from our labeled pixels, the objective function can be defined as:

$$J(\alpha) = \alpha^T L \alpha + \rho(\alpha - \beta)^T D(\alpha - \beta) \tag{7}$$

Here β is a $|P| \times 1$ vector. The value is one if the pixel is labeled as the current target tissue type and zero otherwise. D is a $|P| \times |P|$ diagonal matrix whose elements are one for labeled pixels and zero otherwise. ρ is a weight assigned a relatively large value (e.g., 100).

By minimizing equation (7), we can obtain the value of α, which can be treated as the likelihood of the pixels being the current target tissue type. In this way, we extract the GM, WM and CSF respectively. After that, we obtain three tissue likelihood maps (as shown in Fig. 3). Then we can classify a pixel into GM, WM, CSF according to its maximum likelihood in these three maps.

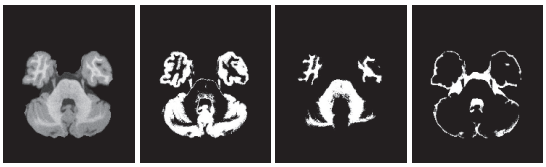

(a) (b) (c) (d)

Figure 3. (a) MRI data after brain extraction. (b) − (d) GM, WM and CSF of our soft segmentation result.

3. Experiments and evaluations

3.1. Test data

We use the dataset from BrainWeb (http://www.bic.mni.mcgill.ca/brainweb/), which is a simulated brain database. The advantage of using this dataset in experiments is the availability of a ground truth (gold standard) for the tissue types from which the MRI data volumes were created. Specifically, the test data in our experiments are six T1-weighted brain MRI volumes. The volume size is $181 \times 217 \times 181$, with voxel resolution $1mm \times 1mm \times 1mm$. The volumes are combined with additive noise ranging from 0% to 9%, and intensity nonuniformity of 40%. Before the experiments, we remove the non-brain structures from the test data with the brain extraction tool in FSL [9].

3.2. Results and evaluations

We compare the results of SPM8 [10], FMRIB's Automated Segmentation Tool (FAST) in FSL [9] and the proposed method with the ground truth of BrainWeb, and compute the Dice metric to quantify the overlap between the segmentation results and the ground truth for each tissue type. Specifically, the Dice metric for tissue t is defined as: $D(t) = 2V_{sg}^t / (V_s^t + V_g^t)$, where V_s^t and V_g^t represent the number of pixels (voxels) assigned to tissue t by the segmentation algorithm and ground truth, respectively. We select 120 successive slices from each volume and compute the average Dice overlap on these slices. The first and last few slices are not selected because there are few corresponding structures in these slices for some tissue types. The values of the Dice overlap may be unstable and affect the statistical analysis. The experimental results are shown in Fig. 4. In Fig. 4(a)−(c), we can see that for GM and CSF, results of our proposed method are more accurate than that of the other two. For WM, ours performs worse when the noise increases. This is because when we determine the initial labeled pixels, we use fuzzy c-means, which is not robust in noisy slices. There may be not enough labeled pixels. Meanwhile we can find that for FAST and SPM8, results of the volumes with a moderate amount of noise are better than that of volumes without noise.

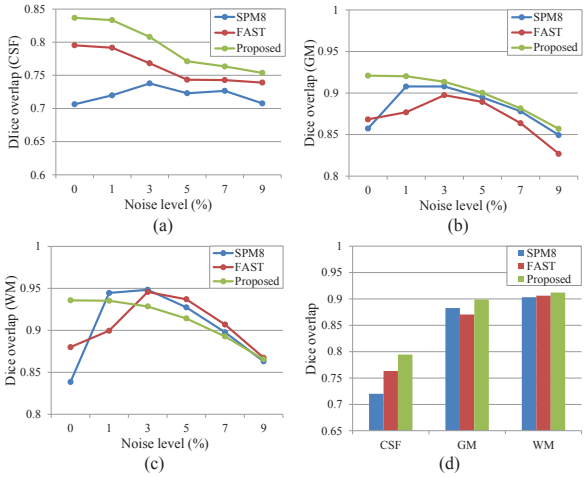

Figure 4. (a)–(c) Average Dice overlap metric of the results from SPM8 [10], FAST [9] and the proposed method. The test MRI volumes are from BrainWeb with different noise levels. (d) Average Dice overlap with all of the test slices.

This is also noted in [12] and probably because of the noise models. In Fig. 4(d) we present the average Dice overlap of the 720 test slices (6 volumes and 120 test slices for each volume) with respect to CSF, GM, WM. It shows that performance of the proposed method is a little higher than that of the competitors on average.

We also evaluate the results visually. Fig. 5 shows the WM and GM segmentation results of SPM8, FAST and our method. Because of the additive noise, all of the methods cause artifacts. However, in the first row, we can see that our result is less noisy. In the second row, there is a tiny amount of WM in the region enclosed by the red rectangle. The tissue homogeneity is also affected by the noise. We can see that results of the three methods can reveal this detail to some extent. Our result is comparable to that of the other two.

4. Conclusions

In this paper, we propose a novel method for segmentation of brain tissue in MRI. We first label some pixels based on spatial prior, and then segment the rest pixels by propagating the label information with the neighboring pixels affinities. The result can be obtained by minimizing a quadratic objective function. The main advantage of our method is that the underlying model can naturally model the partial volume effects. The MRI segmentation is reduced to solving this linear model. Experiments demonstrate that the results of our method are comparable to that of the state-of-the-art methods. Currently, we model the pixel affinity in two-dimension. We may generalize it in the three dimensional space in the future work.

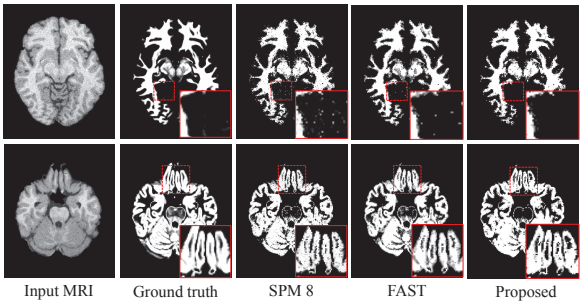

Figure 5. WM, GM Ground truth and segmentation results from SPM8 [10], FAST [9], and the proposed method.

References

[1] J. Ashburner and K. J. Friston. Unified segmentation. *NeuroImage*, 26: 839-851, 2005.

[2] H. Greenspan, A. Ruf, and J. Goldberger. Constrained Gaussian mixture model framework for automatic segmentation of MR Brain Images. *IEEE Trans. Medical Imaging*, 25(9): 1233-1245, 2006.

[3] J. R. Jiménez-Alaniz, V. Medina-Bañuelos, and O. Yáñez-Suárez. Data-driven brain MRI segmentation supported on edge confidence and a priori tissue information. *IEEE Trans. Medical Imaging*, 25(1): 74-83, 2006.

[4] J. V. Manjon, J. Tohka, and M. Robles. Improved estimates of partial volume coefficients from noisy brain MRI using spatial context. *NeuroImage*, 53: 480-490, 2010.

[5] A. Vovk, R. W. Cox, J. Stare, D. Suput, and Z. S. Saad. Segmentation priors from local image properties: without using bias field correction, location-based templates, or registration. *NeuroImage*, 55:142-152, 2011.

[6] Z. Yi, A. Criminisi, J. Shotton, and A. Blake. Discriminative, semantic segmentation of brain tissue in MR Images. *MICCAI*, pp. 558-565, 2009.

[7] J. L. Marroquin, B. C. Vemuri, S. Botello, F. Calderon, and A. Fernandez-Bouzas. An accurate and efficient Bayesian method for automatic segmentation of brain MRI. *IEEE Trans. Medical Imaging*, 21(8): 934-945, 2002.

[8] C. Ciofolo. Atlas-based segmentation using level sets and fuzzy labels. *MICCAI*, pp. 310-317, 2004.

[9] M. W. Woolrich, S. Jbabdi, B. Patenaude, M. Chappell, S. Makni, T. Behrens, C. Beckmann, M. Jenkinson, and S. M. Smith. Bayesian analysis of neuroimaging data in FSL. *NeuroImage*, 45:173-186, 2009.

[10] Statistical parametric mapping (SPM). Available at: http://www.fil.ion.ucl.ac.uk/spm, 2009.

[11] A. Levin, D. Lischinski, and Y. Weiss. A closed form solution to natural image matting. *CVPR*, pp. 61-68, 2006.

[12] A. R. Ferreira da Silva. A Dirichlet process mixture model for brain MRI tissue classification. *Medical Image Analysis*, 11: 169-182, 2007.